Applied Physics A (2020) 126:57
https://doi.org/10.1007/s00339-019-3200-x

Applied Physics A
Materials Science & Processing

S.I.: CURRENT STATE-OF-THE-ART IN LASER ABLATION

Thin films prepared by a hybrid deposition configuration combining two laser ablation plasmas with one sputtering plasma

L. Escobar-Alarcón[1] · D. A. Solis-Casados[2] · S. Romero[1] · E. Haro-Poniatowski[3]

Received: 14 October 2019 / Accepted: 2 December 2019 / Published online: 23 December 2019

Abstract
A hybrid configuration for multicomponent thin film deposition by combining two laser ablation plasmas with one sputtering plasma is presented. This setup was used to deposit TiO_2 thin films modified simultaneously with Bi and Pt. In order to investigate the effect of the metal incorporation in titania the deposited films were characterized by X-ray photoelectron, Raman, UV–Vis and photoluminescence spectroscopies, as well as by X-ray diffraction and scanning electron microscopy. The results showed that films with different load of Bi and Pt were obtained. The amount of these metals has an important effect on the compositional, structural and optical properties of the deposited films. Mixtures of TiO_2 with Bi_2O_3 as well as metallic Bi and Pt are obtained at the highest Pt content. The index of refraction and band gap decrease as the Pt content increases making these films capable to absorb light from the visible region of the solar spectrum with potential applications as photocatalysts to degrade organic pollutants present in wastewaters.

1 Introduction

Plasmas produced by laser ablation and magnetron sputtering have been extensively used for thin film deposition of a wide variety of materials [1, 2]. These techniques have intrinsic advantages for semiconductors thin film deposition that, when used in hybrid configurations allow the growth of composite nanomaterials formed by two oxides with good control of the composition. Furthermore, thin films of oxides modified with metals as dopants or as embedded nanoparticles can also be prepared. The use of hybrid configurations can be very useful since the deposited material is formed by two independent plasmas produced from different targets giving the possibility to vary the plasma parameters independently in a controlled manner. In this way semiconductor thin films with tailored properties can be synthesized. It is worth mentioning that the hybrid deposition technique combining magnetron sputtering with pulsed laser deposition was proposed initially by Voevodin [3] to deposit carbon-based [4] and TiC–Ag [5] composite films. More recently it has been applied to prepare Cr–enriched DLC layers [6] as well as chromium and titanium doped diamond-like carbon films [7]. Additionally, a variant in which the same target is sputtered and ablated simultaneously has also been reported [8]. The preparation of thin films of oxides modified with metals using alternative configurations of laser ablation have been successfully implemented and employed in our group to synthesize Co:TiO_2 [9], Bi:TiO_2 [10], V_2O_5:Ag [11, 12] and TO_2:Zn [13] thin films with good control of the composition as well as good photocatalytic response under solar irradiation. Particularly, thin films of TiO_2 modified with metals, non-metals, as well as with other oxides in a controlled way has been considered as a good alternative to develop high efficiency photocatalysts with some key advantages such as efficient charge separation and band gap narrowing improving their photocatalytic performance using solar light [14]. Specifically, TiO_2 nanopowders compounded with different amounts of Bi have shown that Bi incorporation in the titanium oxide has an important effect on their optical properties making these composite powders capable to absorb light from the visible region of the solar spectrum and consequently improve their catalytic

✉ L. Escobar-Alarcón
luis.escobar@inin.gob.mx

[1] Departamento de Física, Instituto Nacional de Investigaciones Nucleares, Carretera México-Toluca S/N, La Marquesa, CP 52750 Ocoyoacac, Estado de México, México

[2] Universidad Autónoma del Estado de México, Facultad de Química, Paseo Colon Esq. Paseo Tollocan S/N, CP 50120 Toluca, Estado de México, México

[3] Departamento de Física, Universidad Autónoma Metropolitana Iztapalapa, Apdo. Postal 55-534, Mexico City, CDMX, México

performance [15, 16]. Additionally, the combination of a noble metal as Pt with TiO_2 can form a Schottky barrier between the metal and an electronic potential barrier at the metal–semiconductor interface and act as an electron scavenger reducing the photogenerated charge carrier recombination and consequently increasing the photocatalytic response [17]. In this work, and in line with our previous work to investigate alternative deposition techniques to prepare thin films with superior properties, we report on the implementation of an hybrid deposition configuration in which two laser ablation plasmas are combined with one sputtering plasma to prepare TiO_2 thin films modified simultaneously with Bi and Pt.

2 Experimental procedure

A hybrid deposition configuration in which a plasma formed by magnetron sputtering is combined with two plasmas produced by laser ablation was implemented. Figure 1 shows a photograph of the experimental configuration showing the three plasmas generated simultaneously. For this purpose, a Ti plasma was produced by magnetron sputtering in a high purity argon atmosphere. Bi and Pt plasmas were produced ablating simultaneously the corresponding metal targets using the third harmonic of a Nd:YAG laser (355 nm). As a first step titanium thin films were deposited by DC magnetron sputtering onto glass substrates. The deposition chamber was evacuated to a base pressure close to 5×10^{-6} Torr, afterwards it was filled with argon of high purity (99.99) at a working pressure of 1×10^{-2} Torr. Sputtering was produced

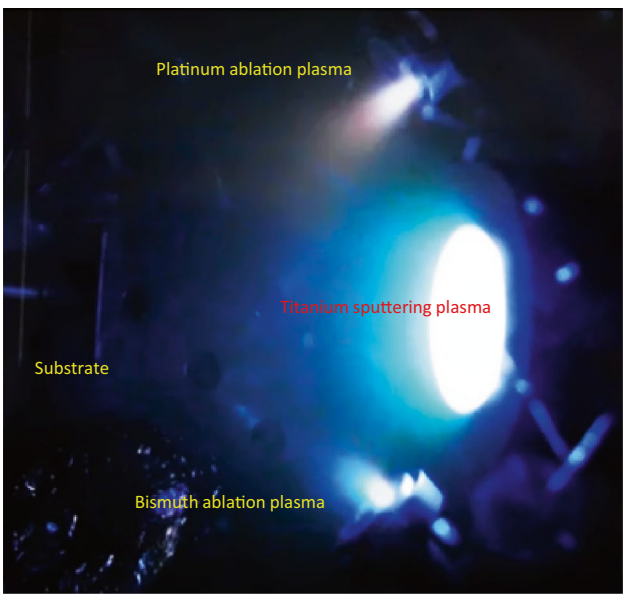

Fig. 1 Photograph of the experimental configuration combining two laser ablation plasmas with a sputtering plasma

generating the plasma using a power of 100 W. The target to substrate distance was set at 7.0 cm and the substrate was kept at room temperature. In order to obtain titanium oxide, the as-deposited thin films were subjected to thermal treatments at temperatures of 450, 500 and 550 °C for 2 h. The optimal temperature was determined to be 550 °C. To produce the laser ablation plasmas, high purity bismuth and platinum targets were ablated simultaneously using the third harmonic of a Nd:YAG laser (355 nm, pulse duration 5 ns, 10 Hz of repetition rate). The Bi target was ablated using a laser fluence close to 3.8 J/cm^2 whereas for the Pt target the laser fluence was close to 10.5 J/cm^2. The target to substrate distance was set at 7 cm and the deposition time was 45 min for all the samples. The laser ablation plasmas propagate in perpendicular directions interacting on the substrate surface placed perpendicular with respect to the line of propagation of the sputtering plasma. In the implemented experimental configuration, the Bi and Pt laser produced plasmas propagate through an argon atmosphere and after in the Ti plasma produced by sputtering. In a first approximation it can be assumed that these two plasmas are expanding in an Argon atmosphere at a pressure of 1×10^{-2} Torr. It is well known that a background gas can be used to thermalize the energetic species in a laser plasma plume because the gas particles affect significantly the plume expansion dynamics. As a result, the plasma is spatially confined and strongly decelerated with the formation of shock waves. Under this condition the dimensions of the plasma plume are much smaller compared to those observed during the expansion in vacuum. Therefore, in order to favor that these plasmas can reach the substrate surface the use of relatively high laser fluences to ablate the bismuth and platinum targets is necessary. Consequently, the use of higher laser fluences to produce laser ablation plasmas results in the formation of more energetic and denser plasmas. Additionally, in order to obtain a homogeneous film, the substrate was rotated during the deposition time. With the purpose of depositing films with different content of Pt, the Ti sputtering plasma and the Bi laser ablation plasma were combined during all the deposition time whereas for the Pt laser ablation plasma the total deposition time was varied following the procedure reported before [13] according with the Table 1.

The effect of the Bi and Pt incorporation in the TiO_2 film on the chemical composition, crystalline structure, optical properties and thickness was investigated. The composition was determined by X-ray photoelectron spectroscopy (XPS) by acquiring spectra in the low and high-resolution regimes with a Jeol JPS 9200 spectrometer. The microstructure of the films was studied by Raman spectroscopy, the spectra were obtained using a micro-Raman LabRam 800 system, equipped with a confocal microscope Olympus BX40 and a 100X objective; the samples were excited using the second harmonic of a Nd:YAG laser (532 nm). Optical properties

Table 1 Pt total number of laser pulses used to prepare the different samples

Sample	Pt total number of laser pulses
TiO_2	–
TiBiPt1	2400
TiBiPt2	4800
TiBiPt3	9600
TiBiPt4	14,400
TiBiPt5	19,200
TiBiPt6	27,000

Table 2 Atomic content of the different samples

Sample	Bi (at.%)	Pt (at.%)	Ti (at.%)	O (at.%)
TiO_2	–	–	37.0	63.0
TiBiPt1	1.2	–	33.5	65.3
TiBiPt2	1.3	–	34.2	64.5
TiBiPt3	0.74	0.37	31.2	67.1
TiBiPt4	0.46	0.50	34.6	64.4
TiBiPt5	0.34	0.67	35.7	63.3
TiBiPt6	0.30	0.89	34.6	64.2

were determined from UV–Vis measurements carried out on a Perkin Elmer lambda 35 spectrophotometer. Photoluminescence properties were studied by PL spectroscopy using a spectrofluorometer (FluoroMax 4, Horiba Jobyn Ivon) equipped with a 150 W Xenon lamp as excitation source. X-ray diffraction (XRD) patterns were obtained with a Bruker AXS D8-discover diffractometer with the Cu Kα radiation ($\lambda = 1.5406$ Å). The surface morphology was observed by scanning electron microscopy (SEM) using a JEOL JSM 6510LV microscope.

3 Results and discussion

3.1 Chemical composition

The atomic contents of the deposited films determined from XPS measurements are shown in Table 2. The Pt content was varied from 0.37 to 0.89 at.% depending on the total number of laser pulses used to ablate the Pt target. The film without Pt and Bi has a composition very close to stoichiometric TiO_2 only with a slightly deficiency in oxygen indicative of the presence of O vacancies. Therefore, the deposition configuration using three plasmas allows the synthesis of TiO_2 thin films with different content of Pt and Bi.

With the purpose of obtaining information about the chemical state of the elements present in the films, these were characterized by XPS. Figure 2 shows the XPS high-resolution spectra of the binding energy regions of: (a) Ti-2*p*, (b) O-1*s*, (c) Bi-4*f* and (d) Pt-4*f*, corresponding to the sample with a Pt content of 0.89 at.%. The XPS spectrum for the Ti-2*p* region (Fig. 2a) reveals a doublet with peaks at 459.1 and 464.9 eV corresponding to Ti in TiO_2 [18]. Figure 2b shows the high-resolution XPS spectra for the O-1*s* region. In this case an asymmetric shape of this peak is observed indicating the presence of different chemical states, its deconvolution shows the presence of peaks at 530.9 and 533.2 eV. The position of the first one agrees well with the one reported for TiO_2 [18], whereas the second one can be related to Bi_2O_3, suggesting the co-existence of a mixture of TiO_2 and Bi_2O_3. Figure 1c shows the region of Bi-4*f* together with the results of the deconvolution process. The peaks at 157.3 and 162.3 eV are assigned, respectively to the binding energies for the $4f_{7/2}$ and $4f_{5/2}$ states of metallic bismuth [19]. The peaks at 159.2 and 164.3 eV correspond to the $4f_{7/2}$ and $4f_{5/2}$ states of Bi_2O_3, respectively [19]. These results reveal that Bi is incorporated as a metal and as an oxide in approximately the same amount. Figure 2d shows the region of Pt-4*f*, again the results of the deconvolution performed are shown. The peaks at 70.8 and 74.4 eV are assigned to the binding energies for the $4f_{7/2}$ and $4f_{5/2}$ states of metallic platinum respectively, whereas the peaks at 73.4 and 75.9 eV could be assigned to the $4f_{7/2}$ and $4f_{5/2}$ states of PtO [20]. In this case a higher amount of metallic Pt than of Pt oxide is present. In summary the XPS results show that the prepared thin films consist of a titania matrix with a mixture of Pt and Bi in metallic form as well as their corresponding oxides, Bi_2O_3 and PtO.

3.2 Microstructural characterization

The Raman spectroscopy results for the different films are shown in Fig. 3a. The spectrum of the TiO_2 film shows peaks at 142, 235, 444 and 609 cm^{-1}, labelled as R, characteristic of the rutile phase [21]. The intensity of the peak at 142 cm^{-1} together with the two weak signals at 397 and 514 cm^{-1}, labelled as A, suggest the presence of the anatase phase. Therefore, this film is formed by a mixture of the anatase and rutile phases of TiO_2. The Raman spectrum of the prepared sample with the lowest amount of Pt (TiBiPt1 sample) shows two intense peaks at 70 and 92 cm^{-1} corresponding to the E_g and A_{1g} first order Raman modes characteristic of rhombohedral bismuth [22, 23]. It is important to note that the Raman spectra of all the samples show the peaks at 444 and 609 cm^{-1} indicating that the rutile phase is present in all the samples. Upon incorporation of Pt, the peaks at 70 and 92 cm^{-1} become less intense until they disappear completely as it is clearly seen in Fig. 3b. These results reveal that films with a maximum Pt content close to 0.37 at.% consist of a mixture of rutile TiO_2 and metallic bismuth. Further increase of Pt content (> 0.5 at.%) results

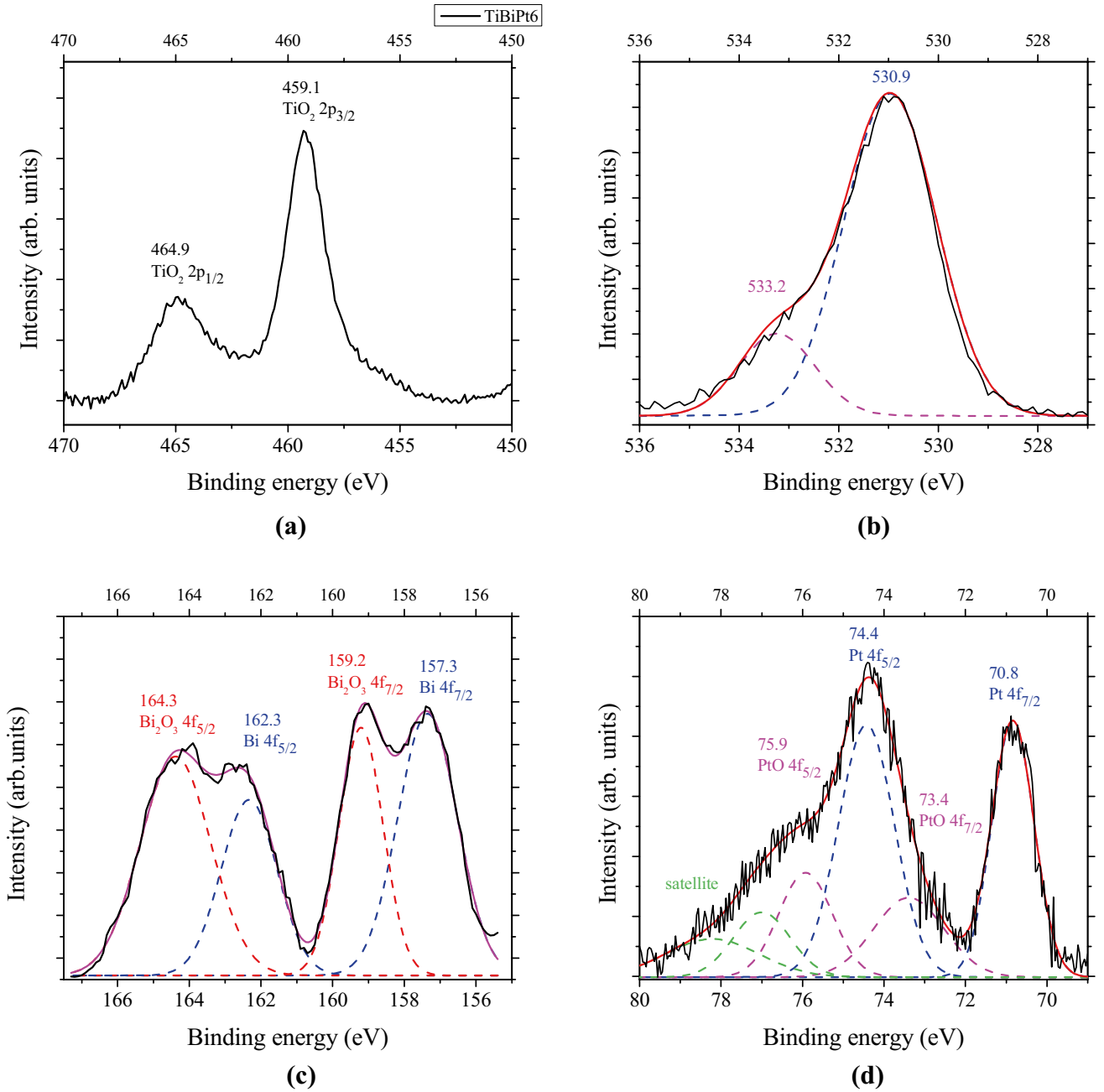

Fig. 2 XPS high-resolution spectra of the binding energy regions of: **a** Ti-2*p*, **b** O-1*s*, **c** Bi-4*f* and **d** Pt-4*f*, of the sample TiBiPt6

in the appearance of peaks at 70, 83, 94, 119, 128, 139, 278 and 320 cm^{-1} as is shown in Fig. 3c. These agree well with the Raman peaks of the α-Bi_2O_3 (monoclinic) phase [24], indicating that at this Pt content the formation of this bismuth oxide is promoted, and the films are formed by a mixture of rutile TiO_2 and α-Bi_2O_3.

Figure 4 shows the X-ray diffraction patterns of films with different Pt content. The sample without Pt and Bi display diffraction peaks at 27.4°, 36.1°, 41.2° and 54.3° corresponding to the rutile phase of TiO_2 (JCPDS 01-083-2242). This phase is present for all samples no matter the Pt or Bi content. The X-ray diffraction pattern of the sample with 1.3 at.% of Bi (sample TiBiPt-2) shows diffraction lines at 22.6°, 22.9°, 32.7°, 39.7°. These lines can be attributed to Bi_2O_3 (JCPDS 01-074-2351) indicating that mixtures of rutile TiO_2 and bismuth oxide are obtained for this sample. At 0.5 at.% of platinum content (sample TiBiPt-4) no diffraction peaks corresponding to Bi oxide were observed. In this case, additionally to the peaks assigned to rutile, two new signals are observed at

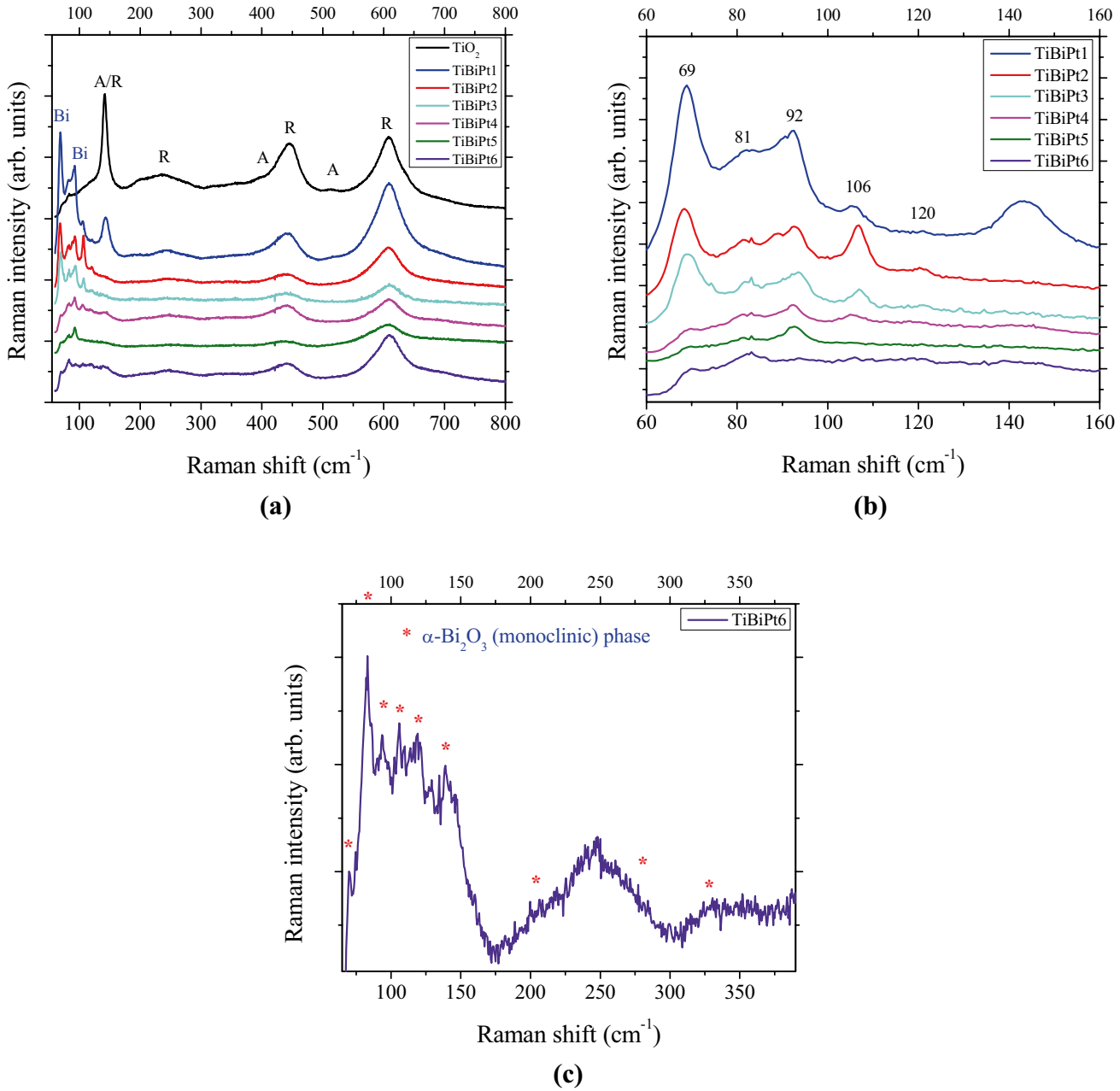

Fig. 3 **a** Raman spectra of the different samples with various Bi and Pt contents, **b** zoom of the low frequency region, **c** Raman spectrum of the sample with the highest Pt content

30.83° and 40.10° which can be attributed to the Bi_2Pt alloy (JCPDS 03-065-9704). Similar results were found for the sample TiBiPt-6. Therefore, XRD results reveal that mixtures of TiO_2 and Bi_2O_3 are obtained when Bi and Pt are incorporated into the films. In general terms these results are consistent with those found by Raman spectroscopy.

3.3 Optical properties

The UV–Vis transmittance spectra of the deposited films are presented in Fig. 5. The incorporation of Bi and Pt has two important effects on the optical transmittance: first, the absorption edge shifts to longer wavelengths as the amount of Pt is increased, indicative of a band gap narrowing;

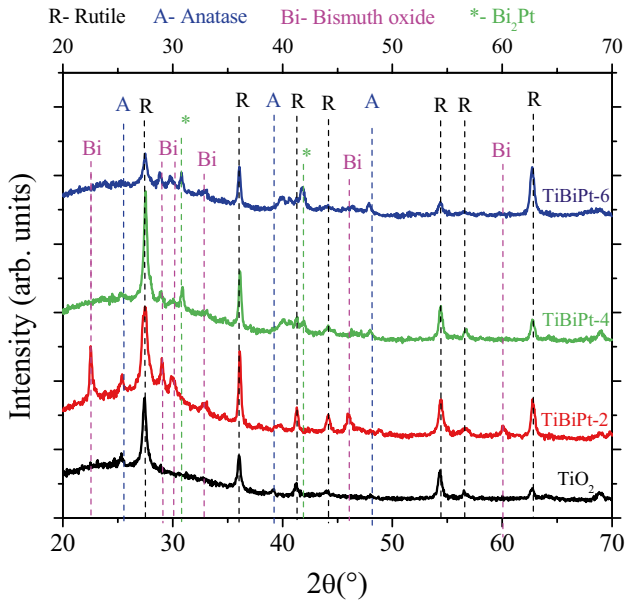

Fig. 4 X-ray diffraction spectra of films with different Bi and Pt contents

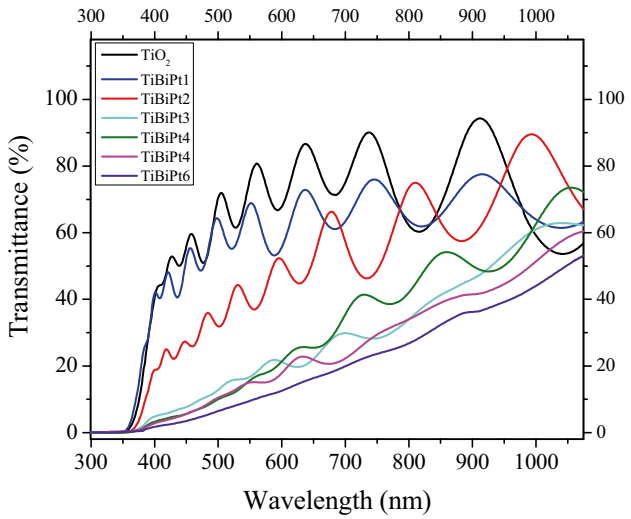

Fig. 5 Transmittance spectra obtained by UV–Vis spectroscopy of the different samples

second, the transmittance decreases dramatically as the amount of Pt increases. Another obvious feature of the transmittance spectra is the presence of maxima and minima, due to interference effects, from which the thickness and refractive index can be determined using the model of Goodman [25]. Thicknesses were found to vary from 806 to 1287 nm while the index of refraction decreases from 2.4 to 1.8 as the Pt content increases. The band gap was determined using the Tauc method assuming direct transitions [26]. This was done by plotting $(\alpha h\nu)^2$ as a function of $h\nu$. The optical absorption

Table 3 Thickness and optical properties of the samples with different Pt content

Sample	Thickness (nm)	Refractive index	Band gap (eV)
TiO_2	806	2.4	2.94
TiBiPt1	963	2.3	3.20
TiBiPt2	1054	2.1	2.88
TiBiPt3	1287	2.0	2.61
TiBiPt4	1590	1.8	2.10
TiBiPt5	[a]	[a]	[a]
TiBiPt6	[a]	[a]	[a]

[a]Not possible to calculate

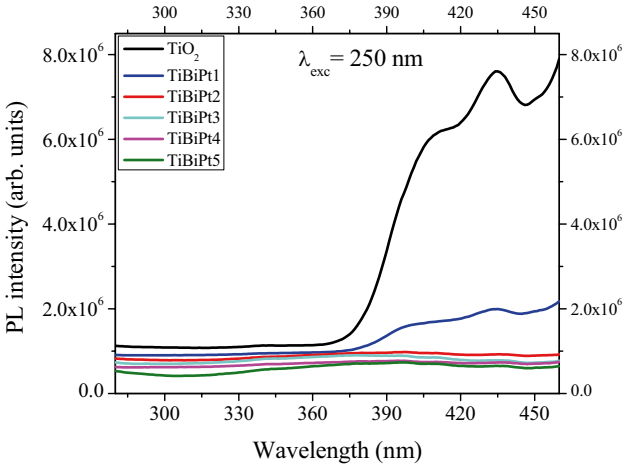

Fig. 6 Photoluminescence spectra of the samples with different Bi and Pt contents

coefficient was obtained using the expression: $\alpha = -\ln(T)/t$, where t is the thickness of the film and T the transmittance. It was found that further increase of Pt content decreases the band gap to values as low as 2.10 eV. These results are summarized in Table 3.

A potential application of the prepared thin films is as photocatalysts in order to degrade persistent organic pollutants in wastewaters. For this application a key issue is to investigate the generation, separation, and recombination of photogenerated electron–hole pairs since they are responsible for the formation of hydroxyl radicals, the active specie to degrade until the complete mineralization of organic molecules. The photoluminescence (PL) spectra shown in Fig. 6 were measured at 250 nm excitation wavelength. The TiO_2 film exhibit an intense band peaking at 408 and 435 nm (3.03 and 2.85 eV) that can be attributed to near band edge emissions in good agreement with the band gap value determined previously. This intense PL signal indicates high photogenerated charge

recombination. When Pt and Bi are incorporated in the films, a strong quenching of the PL emission is clearly observed. This can be attributed to the presence of Bi and Pt metallic nanoparticles that favor a better charge separation as electrons generated in the conduction band of the TiO_2 are trapped by these metal nanoparticles. As more metal is incorporated in the film the charge separation and the quenching of the PL intensity are increased as it is seen in Fig. 6. The relative higher electron–hole recombination rate in the TiO_2 film could be associated with a lower degradation degree of organic molecules whereas a higher degradation degree is expected with the films containing bismuth and platinum. Further studies regarding this potential application are underway.

3.4 Surface morphology

The surface morphology of the deposited films is observed in the SEM images shown in Fig. 7. The film without Bi and Pt shows a surface formed by grains with dimensions in the nanometric scale revealing a nanostructured surface. The Bi and Pt incorporation changes the morphology, producing spherical particles with lengths about 1 μm as can be seen in Fig. 7a. Further increase in platinum content promotes an increase in the size of the spherical particles to 1.6 μm in average, additionally a greater number of such particles is also observed. Elemental atomic composition of the film surface as well as of the spherical particles determined by the EDS analysis, reveal the same composition for both.

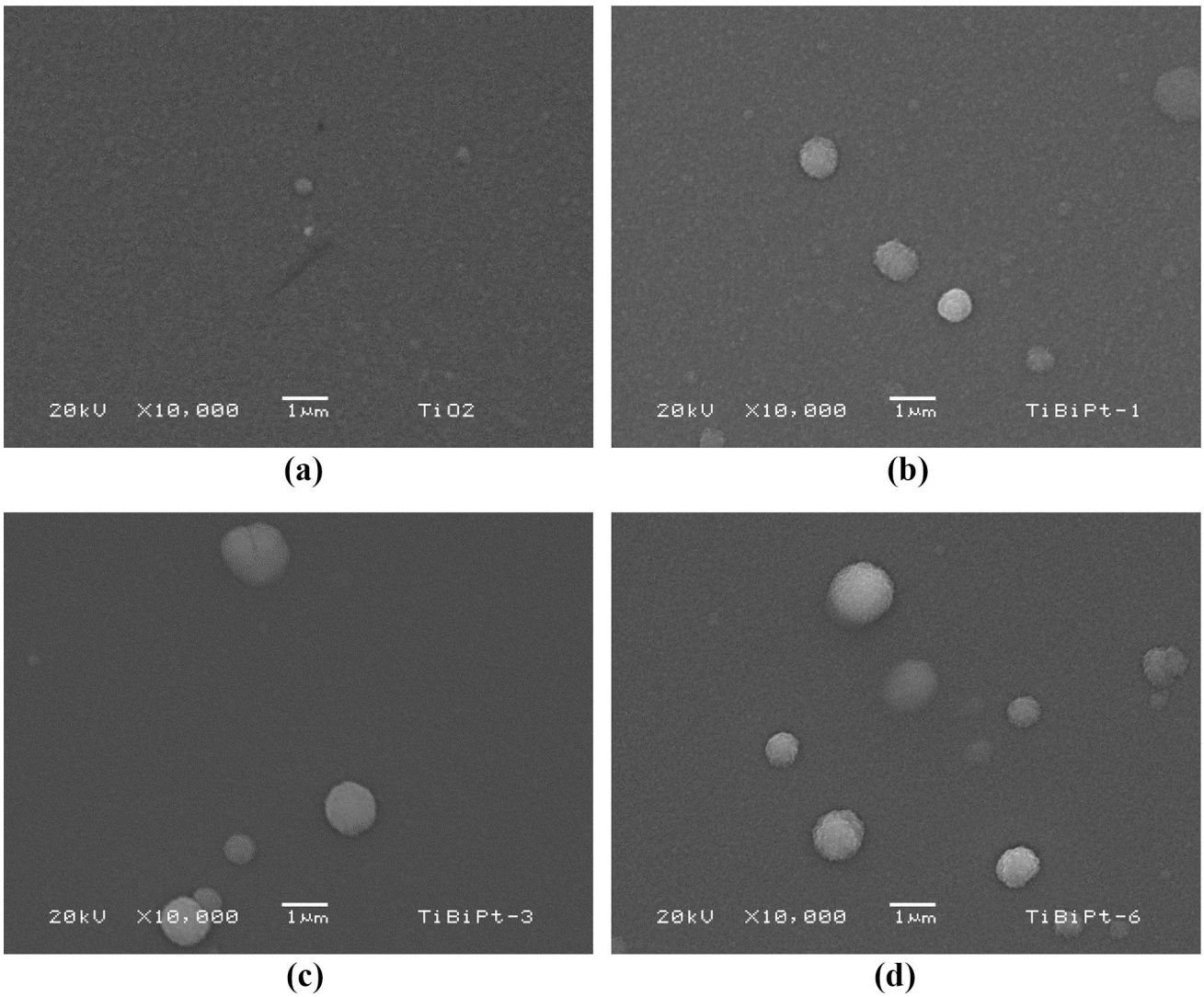

Fig. 7 Surface morphology of the different deposited films

4 Conclusions

Titania thin films with different content of Pt and Bi were obtained by combining two laser ablation plasmas with one sputtering plasma. The characterization of the prepared samples indicates the presence of Bi and Pt in metallic form as well as their respective oxides. The band gap energy decreased with increasing Pt concentration from 2.94 eV for pure TiO_2 to 2.10 eV for the sample with 0.50 at.% of Pt making these films capable to absorb light from the visible region of the solar spectrum. The incorporation of Pt on TiO_2 seems to favor the separation of photogenerated charges reducing the recombination. An important advantage of the implemented experimental configuration lies in the fact that the three plasmas are produced and controlled independently allowing the possibility to vary the plasma parameters individually in a controlled manner and therefore multicomponent thin films with tailored properties can be prepared.

Acknowledgements This research was partially supported by the CONACYT project CB-240998.

References

1. D.B. Chrisey, G.K. Hubler, *Pulsed Laser Deposition of Thin Films* (Wiley, New York, 1994)
2. P.J. Kelly, R.D. Arnell, Vacuum **56**, 159 (2000)
3. A.A. Voevodin, M.A. Capano, A.J. Safriet, M.S. Donley, J.S. Zabinski, Appl. Phys. Lett. **69**, 188 (1996)
4. A.A. Voevodin, J.P. O'Neill, S.V. Prasad, J.S. Zabinski, J. Vac. Sci. Technol. A **17**, 986 (1999)
5. J.L. Endrino, J.J. Nainaparampil, J.E. Krzanowski, Surf. Coat. Technol. **157**, 95 (2002)
6. M. Jelinek, J. Zemek, M. Vandrovcová, L. Bačáková, T. Kocourek, J. Remsa, P. Písařík, Mater. Sci. Eng. C **58**, 1217 (2016)
7. M. Jelínek, J. Zemek, J. Remsa, J. Miksovsky, T. Kocourek, P. Písarík, M. Trávnícková, E. Filová, L. Bacáková, Hybrid laser technology and doped biomaterials. Appl. Surf. Sci. **417**, 73 (2017)
8. D. Benetti, R. Nouar, R. Nechache, H. Pepin, A. Sarkissian, F. Rosei, J.M. MacLeod, Sci. Rep. **7**, 2503 (2017)
9. L. Escobar-Alarcón, J. Álvarez, D.A. Solís-Casados, E. Camps, S. Romero, J. Becerril, Appl. Phys. A **110**, 909 (2013)
10. L. Escobar-Alarcón, D.A. Solís-Casados, S. Romero, J.G. Morales-Méndez, E. Haro-Poniatowski, Appl. Phys. A **117**, 31 (2014)
11. F. Gonzalez-Zavala, L. Escobar-Alarcón, D.A. Solís-Casados, C. Rivera-Rodríguez, R. Basurto, E. Haro-Poniatowski, Appl. Phys. A **122**, 461 (2016)
12. F. Gonzalez-Zavala, L. Escobar-Alarcón, D.A. Solís-Casados, S. Romero, M. Fernández, E. Haro-Poniatowski, E. Castellón, Catal. Today **305**, 102 (2018)
13. L. Escobar-Alarcón, F. Gonzalez-Zavala, D.A. Casados, S. Romero, J. Aspiazu, E. Haro-Poniatowski, Appl. Phys. A **124**, 358 (2018)
14. S. Rehman, J. Hazard. Mater. **170**, 560 (2009)
15. D.A. Solís-Casados, L. Escobar-Alarcón, A. Arrieta-Castañeda, E. Haro-Poniatowski, Mater. Chem. Phys. **172**, 11 (2016)
16. D.A. Solís-Casados, L. Escobar-Alarcón, V. Alvarado-Pérez, E. Haro-Poniatowski, Int. J. Photoenergy, **2018**, Article ID 8715987 (2018)
17. W. Y. Teoh, L. Mädler, R. Amal, J. Catal. **251**, 271 (2007)
18. U. Diebold, T.E. Madey, Surf. Sci. Spectra **4**, 227 (1996)
19. V.S. Dharmadhikari, S.R. Sainkar, S. Badrinarayan, A. Goswami, J. Electron Spectrosc. Relat. Phenom. **25**, 181 (1982)
20. E. Mazzotta, S. Rella, A. Turco, C. Malitesta, RSC Adv. **5**, 83164 (2015)
21. L. Escobar-Alarcón, E. Haro-Poniatowski, M.A. Camacho-Lopez, M. Fernández-Guasti, J. Jarquin, A. Sanchez-Pineda, Surf. Eng. **15**, 411 (1999)
22. K. Trentelman, J. Raman Spectrosc. **40**, 585 (2009)
23. E. Haro-Poniatowski, M. Jouanne, J.F. Morhange, M. Kanehisa, R. Serna, C.N. Afonso, Phys. Rev. B **60**, 10080 (1999)
24. L. Kumari, J.-H. Lin, Y.-R. Ma, J. Phys. D Appl. Phys. **41**, 025405 (2008)
25. A.M. Goodman, Appl. Opt. **17**, 2779 (1978)
26. J. Tauc, R. Grigorovici, A. Vancu, Phys. Status Solidi **15**, 627 (1966)